ness of the tungsten layer deposited on the exposed silicon.

Auger analysis of a phosphoric-acid-treated, thermally grown oxide failed to reveal phosphorus remaining on the surface; the detection limit was below about 10^{14} cm^{-2}. Similarly, no phosphorus was detected on an unoxidized, phosphoric-acid-treated silicon surface.

Summary

Selective tungsten films have been deposited using different insulators important in IC technology to inhibit nucleation. Nuclei form more readily on nitrogen-containing films than on silicon-dioxide films. The presence of phosphorus on the surface tends to inhibit nucleation. The phosphorus can be added either by a surface treatment subsequent to insulator formation or during deposition of the insulator; however, the inhibiting effect is greater in the latter case. These results demonstrate that proper choice of an insulator and its surface treatment immediately before tungsten deposition can allow thicker selective tungsten layers to be formed without nucleation on the surrounding insulating surfaces.

Acknowledgment

The authors would like to thank H. Birenbaum, J. Soto, and J. Turner for experimental assistance, Dr. S. Y. Chiang for encouragement during this investigation, and Dr. D. Coulman for Auger analysis.

Manuscript submitted Oct. 4, 1985; revised manuscript received Dec. 30, 1985. This was RNP 584 presented at the Las Vegas, Nevada, Meeting of the Society, Oct. 13-18, 1985.

Hewlett-Packard Laboratories assisted in meeting the publication costs of this article.

REFERENCES

1. N. E. Miller and I. Beinglass, *Solid-State Technol.*, **25**(12), 85 (1982).
2. E. K. Broadbent and C. L. Ramiller, *This Journal*, **131**, 1427 (1984).
3. K. C. Saraswat, in "VLSI Science and Technology," W. M. Bullis and S. Broydo, Editors, p. 409, The Electrochemical Society Softbound Proceedings Series, Pennington, NJ (1984).
4. I. Beinglass, Private communication.
5. W. A. P. Claassen and J. Bloem, *This Journal*, **127**, 194 (1980).
6. W. A. P. Claassen and J. Bloem, *ibid.*, **127**, 1836 (1980).
7. J. J. Cuomo, in "Proceedings of the 3rd International Conference on Chemical Vapor Deposition," F. A. Glaski, Editor, p. 270, American Nuclear Society, Salt Lake City, UT, April 24-27, 1972.

Etching Profiles at Resist Edges

I. Mathematical Models for Diffusion-Controlled Cases

H. K. Kuiken, J. J. Kelly, and P. H. L. Notten

Philips Research Laboratories, 5600 JA Eindhoven, The Netherlands

ABSTRACT

Mathematical models are presented that describe diffusion-controlled etching near resist edges. To understand the role of the various physical parameters, a simple maskless one-dimensional model is studied first. The study of a purely diffusion-controlled case suggests that mathematical models for etching problems may be solved by means of perturbation techniques that assume relatively small displacements of the etching surface. The perturbation procedure is then applied to a two-dimensional problem that involves a mask. Assuming a stationary etchant and diffusion control, it is shown that etch rates are largest close to the resist edge. As a result, the etching profile reveals a bulging shape near the mask edge, confirming earlier observations reported in the literature. A case with convection is considered next. It is shown that the very same bulge that resulted from the analysis of the stationary case may also appear when convection plays a role. The perturbation procedure depends upon an important dimensionless parameter β. Tabulated values of this parameter for various etching systems are presented.

Etching of special forms and profiles using resist patterns is often of essential importance in device technology. Two typical examples are shown in Fig. 1. Forms with symmetrical rounded edges or V-shaped grooves are widely used in laser applications. Since the dimensions of such structures are on a micron scale, the accuracy and reproducibility of the etched profiles are critical.

Very often, differences in etching kinetics can be exploited to achieve specific effects. Etching results depend markedly on whether the dissolution reaction is surface(kinetically)-controlled or diffusion-controlled. For example, kinetically controlled etching of anisotropic material frequently gives a faceted surface structure (Fig. 1(a)), characteristic of the crystal properties of the material (1, 2). This results from differences in etch rate of the various crystal planes. The geometric aspects of this kind of etching can be described by Wulff plots (1).

In diffusion-controlled etching, on the other hand, the dissolution rate is determined by transport of active etching components to the solid surface (or of reaction products away from the surface). In the limiting case, the surface reaction proceeds infinitely fast, irrespective of the crystallographic orientation. The amount of active material reaching (or leaving) the surface per unit time obviously determines the etch rate in this case. Etching might, therefore, be expected to be isotropic (2), even in the case of anisotropic materials (Fig. 1(b)).

For kinetically controlled processes, the shape of the etched surface can, in principle, be deduced directly from kinetic and geometric considerations. For diffusion-controlled dissolution, this is only possible on the basis of a complete description of the concentration field in the etching solution. In the context of etching, such multidimensional concentration fields have only recently received any attention (3, 4, 5). However, the form of etched structures can only be studied theoretically by considering models that refer to more than one dimension. This is particularly evident in the case of mask etching, when part of the surface is protected by a resist layer. In the vicinity of the mask edge, the concentration field will be at least two-dimensional, as will be the shape of the etched surface.

In this paper, we present a mathematical model for diffusion-controlled etching of a semi-infinite solid partly covered by a protecting mask. It is known that, in such a case, the etch rate near the mask edge is considerably enhanced (6, 7, 8). While the role of mass transport in solution has been recognized, no previous attempt has been made to predict such etched profiles theoretically. This is probably due, in part, to the mathematical complexity

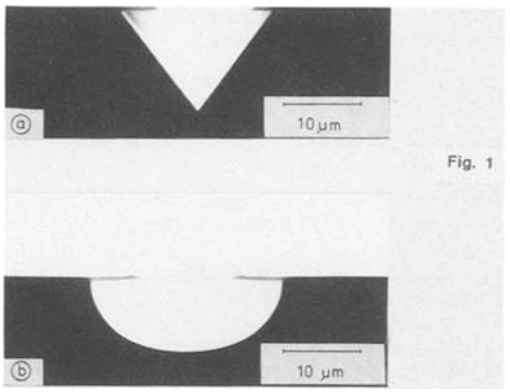

Fig. 1

Fig. 1. Examples of kinetically controlled (a) and diffusion-controlled (b) etching of the same material (GaAs).

of the problem. To introduce the physical parameters that play a role in the mathematical description of etching processes, we first use a simple one-dimensional diffusion model based on the chemical etching of GaAs. In the subsequent two-dimensional mathematical treatment, the influence of both diffusion and convection on the etched profile is considered.

In the second paper of this series (9), experimental results for the etching of III-V materials will be presented and compared with those predicted by theory.

Chemical Etching

As a simple example, we allow a III-V material AB to react chemically with a molecule X_2 from aqueous solution in a series of consecutive steps (10)

$$\begin{array}{c} \diagdown \quad \diagup \\ \text{A—B} \\ \diagup \quad \diagdown \end{array} + X_2 \xrightarrow{k_s} \begin{array}{c} \diagdown \quad \diagup \\ \text{A} \quad \text{B} \\ \diagup \quad \diagdown \end{array} \qquad \begin{matrix} \text{X} & \text{X} \\ | & | \end{matrix} \qquad [1]$$

$$\begin{array}{c} \diagdown \quad \diagup \\ \text{A} \quad \text{B} \\ \diagup \quad \diagdown \end{array} + 2X_2 \xrightarrow{\text{fast}} AX_3 + BX_3 \quad \text{(in solution)} \qquad [2]$$

We assume that the breaking of the first A-B bond at the surface (step 1) is rate-determining (10). In chemical dissolution, the rate constant k_s does not depend on the electric field of the space-charge layer in the solid or of the double-layer in solution. Consequently, the chemical etch rate is not changed if an external potential is applied to the solid (10, 12). The value of k_s can, of course, depend on crystallographic orientation for anisotropic materials. The dissolution products, AX_3 and BX_3, may be subsequently hydrolyzed in solution. From reactions [1] and [2], it is clear that the rate j_s at which the solid dissolves depends on the concentration of X_2 at the solid surface

$$j_s = k_s c_x{}^0{}_2 \qquad [3]$$

For the chemical dissolution of III-V materials, the model system in the present work, bifunctional molecules are required as active etching agent: Br_2, I_2, and H_2O_2 have been used for GaAs (10, 11, 13), and HCl for InP (12).

One-Dimensional Model

In this section, we develop a one-dimensional mathematical model for an etching process such as that described above. In order to emphasize the influence of the various physical parameters, the etchant is first assumed to be stationary, *i.e.*, convection effects are disregarded. Of course, in a real etching process, where one considers diffusive transport through a liquid, convection can hardly ever be left out of consideration. As is shown in (14), convection is negligible only during the very first stages of the process, when the diffusion layer is still very thin.

Convection effects considerably complicate the mathematical modeling of etching processes. Indeed, any relevant model will have to be at least two-dimensional. These two-dimensional models will be considered later. Therefore, the results obtained in this section should be seen as the necessary initial steps toward more sophisticated models.

Figure 2 shows a one-dimensional continuum that is partly occupied by the solid (AB) to be etched, the remaining part being filled with etching liquid. The continuum is measured by the coordinate y, which assumes the value zero at the initial ($t = 0$) position of the interface. At any subsequent time, the location of the interface is denoted by $y = -\delta$. Assuming, as we did in the previous section, that it is sufficient to consider the diffusion of only one species (X_2), the concentration of which will be denoted by c (mol/m³), we apply Fick's second law of diffusion in the region $y > -\delta$

$$\frac{\partial c}{\partial t} = D \frac{\partial^2 c}{\partial y^2} \qquad (t \geq 0,\ y > -\delta) \qquad [4]$$

where t is the time and D (m²/s) is the diffusion coefficient. The initial condition is

$$c = c^b,\ \delta = 0 \text{ at } t = 0 \qquad [5]$$

the first of the two conditions prevailing for all $y \geq 0$. Subsequently, the bulk concentration c^b will be approached at a sufficiently large distance from the interface, *i.e.*

$$c \to c^b \text{ when } y \to \infty\ (t > 0) \qquad [6]$$

The rate of the surface reaction, as described by Eq. [3], must be equal to the flux of the active etching component at the surface, *i.e.*

$$D \frac{\partial c}{\partial y} = k_s c \qquad \text{at } y = -\delta(t) \qquad (t > 0) \qquad [7]$$

Further, since $-d\delta/dt$ is the inward-directed velocity at which the interface proceeds into the solid, a simple mass balance shows that

$$\frac{d\delta}{dt} = \sigma_e \frac{\partial c}{\partial y} \qquad \text{at } y = -\delta\ (t > 0) \qquad [8]$$

where σ_e is given by

$$\sigma_e = \frac{DM_s}{m\rho_s} \qquad [9]$$

Here, M_s is the molecular weight of the solid, ρ_s is its density, and m represents the number of molecules of active etching component required to dissolve one molecule of the solid. The subscript e is chosen to emphasize that we are dealing with an etching system.

Diffusion-controlled etching.—The system of Eq. [4]-[8] assumes a simpler form in the limit of diffusion-controlled etching. In that case, the surface reaction can be thought to occur at an infinite rate, *i.e.*, $k_s = \infty$. The condition of Eq. [7] can then be replaced by

$$c = 0 \text{ at } y = -\delta\ (t > 0) \qquad [10]$$

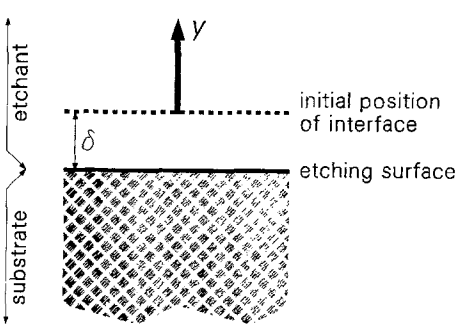

Fig. 2. Geometry for one-dimensional etching. Shaded region: substrate or solid. Case depicted refers to a case where a slice of thickness δ has been etched away.

The problem defined by Eq. [4]-[6], [8], and [10] is well known in applied mathematics literature. It was first formulated in connection with the melting of ice. It belongs to the so-called class of Stefan problems, named after one of the first investigators of the field (15, 16). The solution can be written as follows

$$c = c^b \int_{-\gamma}^{y/2(Dt)^{1/2}} e^{-p^2} dp \Big/ \int_{-\gamma}^{\infty} e^{-p^2} dp \qquad [11]$$

where γ is a constant that is implicitly given by

$$2\gamma e^{\gamma^2} \int_{-\gamma}^{\infty} e^{-p^2}\, dp = \frac{1}{\beta} \qquad [12]$$

and where

$$\beta = \frac{D}{\sigma_e c^b} \qquad [13]$$

This dimensionless parameter β was first introduced in connection with etching in Ref. (3). Figure 3 shows γ as a function of β.

From the presentation of the solution as an integral [11] with the coordinate y appearing in the upper bound, it follows that the position of the moving interface ($y = -\delta$) is obtained by equating upper and lower bounds. In that case, Eq. [11] assumes the value zero, as it should according to Eq. [10]. This yields

$$\delta = 2\gamma(Dt)^{1/2} \qquad [14]$$

from which it is seen that the interface displacement is directly proportional to the square root of the time. The velocity at which the interface moves is defined by [8] and is inversely proportional to the square root of the time. This corresponds to the Cottrell equation (17) for current transients in electrochemical processes. Figure 4 shows, for a special case, how the concentration profile changes with time. Figure 5 presents the dependence of the concentration profile on β, as expressed in dimensionless coordinates.

The dimensionless parameter β defined by Eq. [13] appears to be important in the mathematical description of etching processes. Referring to Eq. [9], we find that β may be written as follows

$$\beta = \frac{m\rho_s}{c^b M_s} \qquad [15]$$

Once the essential chemical or electrochemical reaction determining a particular etching process is known, one may calculate β from the known values of the physical quantities that appear on the right-hand side of [15]. We have done so for a few well-known etching systems, both chemical and electroless. The results are listed in Table I. From the values collected in this table, it follows that β is usually a very large parameter.

A useful result follows when β is large. Indeed, from Fig. 3, the parameter γ is then seen to be of the order of β^{-1}. Since this is the case, Eq. [14] shows that the displacement of the moving boundary is small in comparison with the extent of the diffusion field (Fig. 5), as expressed by the diffusion length $(Dt)^{1/2}$.

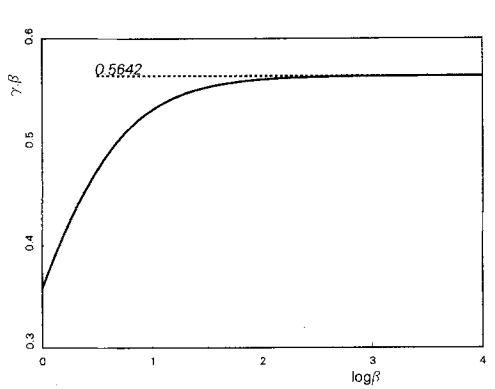

Fig. 3. Etching depth parameter γ (Eq. [14]) as a function of the etching parameter β (Eq. [13] and [15]). (Showing the product $\gamma\beta$ produces a better picture than γ vs. β.)

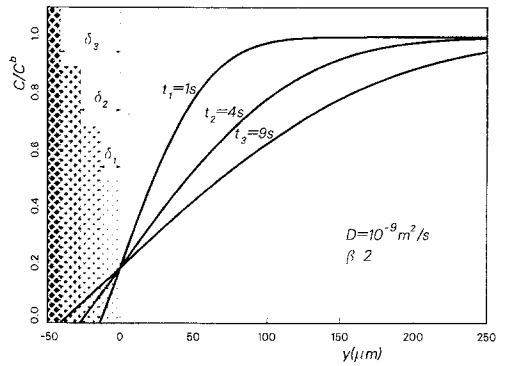

Fig. 4. Sketch showing how the concentration profile develops as the etching boundary moves inwards. The various stages of the solid are shown symbolically using different shadings and heights.

Perturbation method.—The moving boundary problem described above is the only one among those referring to physical situations, real or idealized, that can be solved exactly (16). This means that, in all other cases, we have to resort to approximate methods of solution. Because of this, it is of great value that we have found the dimensionless parameter β to be generally much larger than unity, which corresponds to relatively small displacements of the moving boundary. Any problem satisfying this condition may be solved by means of a so-called perturbation technique. Here, the first step in this procedure is to assume that the etching surface stays put in its original position, which is at $y = 0$, and to calculate the resulting diffusion field. The idea behind this is that the field will change only slightly when relatively minor surface displacements occur. The surface-concentration gradient, in particular, is not expected to be affected a great deal by these minute boundary shifts. The second step in the perturbation procedure is the substitution of the surface-concentration gradient in [8]. Integrating the resulting equation, we obtain a good approximation to the surface displacement. This procedure may be continued to obtain ever better approximations. However, for all practical purposes, one may leave it after these first two steps, particularly when β is as large as, or larger than, say, 100. The power of the method is clearly demonstrated in the case of two-dimensional problems, examples of which will be considered next.

Two-Dimensional Model

Etching in a stagnant medium.—It is the purpose of this section to show how the perturbation technique may

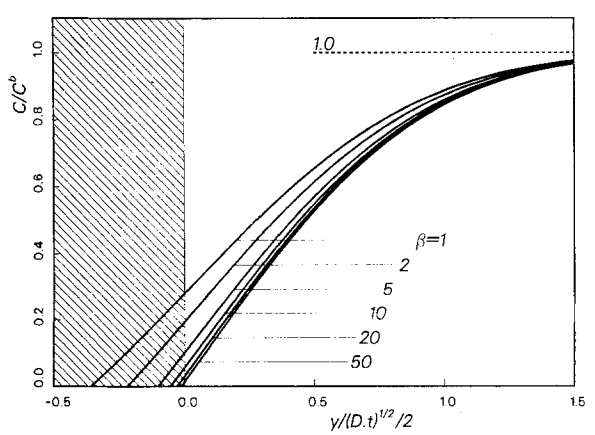

Fig. 5. Sketch showing normalized (c/c^b) concentration profiles as functions of the distance from the initial position of the interface (y) rendered dimensionless by means of the diffusion length $(Dt)^{1/2}$. Picture shows that the ratio of the etching depth and the diffusion-layer thickness becomes smaller and smaller as β increases.

Table I. β values for some typical etching systems

Solid	Etchant	Rate-determining Species	Concentration	m	β	Reference
GaAs	$K_3Fe(CN)_6$ pH 14	$Fe(CN)_6^{3-}$	0.1M	6	2200	(9)
	$K_3Fe(CN)_6$ pH 12	OH^-	0.01M	10	37000	(9), (26)
	$HCl:H_2O_2:H_2O$ = 80:4:1	H_2O_2	0.46M	3[a]	240	(9)
	= 160:4:1	H_2O_2	0.24M	3[a]	460	(9)
InP	Br_2/CH_3OH	Br_2	0.1M	3[a]	1000	(27)
	HCl/acetic acid	HCl	1.0M	3	100	(12)
Fe	$FeCl_3$/HCl	Fe^{3+}	0.1M	2	2800	(3)
Al	$K_3Fe(CN)_6$ pH 14	$Fe(CN)_6^{3-}$	0.1M	3	300	(28)
SiO_2	HF/NH_4F	HF	1.0M	6	230	(29)

[a] Values assumed (not known experimentally).

be applied to a two-dimensional problem. Disregarding convection for the moment, we apply Fick's second law of diffusion in two dimensions

$$\frac{\partial c}{\partial t} = D\left(\frac{\partial^2 c}{\partial x^2} + \frac{\partial^2 c}{\partial y^2}\right) \qquad [16]$$

where t is the time, and x and y constitute a Cartesian coordinate system that will be defined presently. It is again assumed that the etching process is fully determined by the diffusive transport of the active etching component, the concentration of which is denoted by c.

The problem involves a semi-infinite solid etched by a solution that fills the remaining (semi-infinite) part of space (see Fig. 6). The surface of the solid is partly covered with a mask that prevents contact with the etchant. This mask is assumed to be semi-infinite. Along the remaining part of the solid boundary, the etchant is in contact with the solid. The coordinate x measures distance along the bounding plane. At an initial time $t = 0$, the interface is in the plane $y = 0$. However, owing to the etching process itself, the interface is not stationary. At later times, it will be found somewhere below the plane $y = 0$. It is the object of the mathematical model to predict the shape of the interface at any time beyond $t = 0$.

It should be emphasized that the notion of "infinity" is merely a mathematical abstraction. What is really meant by this term is that the system observed is large in comparison with a length characterizing the etching process. In a purely time-dependent diffusive system, this length is the diffusion length $(Dt)^{1/2}$. For the system considered here, a typical value of D is 10^{-9} m^2/s. If such a purely diffusive system could be maintained for the duration of the actual etching process, which lasted, say, a thousand seconds, the diffusion length would be of the order of one millimeter. In that case, a system with a size of only a few centimeters could be considered as infinitely large. Of course, when convection plays a role, a different characteristic length will have to be used.

We need boundary conditions in addition to the field Eq. [16]. First, $c \to c^b$ at distances far away from the solid boundary. The same conditions holds everywhere in $y > 0$ at $t = 0$. Since there is no chemical reaction of any kind on the mask, the normal gradient of c must be zero there,

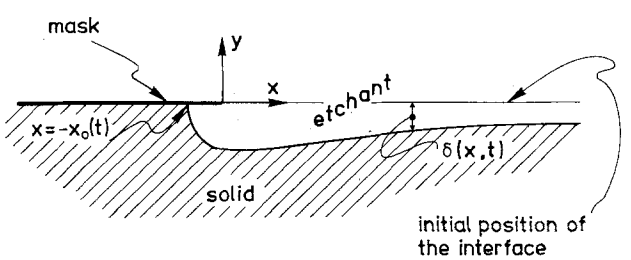

Fig. 6. Geometrical configuration for the etching of a semi-infinite medium covered with a semi-infinite mask. Picture shows the tentative shape of the interface after etching.

i.e., $\partial c/\partial y = 0$. This condition also applies at the underside of the mask when this has been etched free. It should be noted that, in our model, the mask is assumed to be infinitely thin. This is a valid idealization when etching depths are considered that are much larger than the actual thickness of the mask.

To complete our set of boundary conditions we must consider what happens at the interface. The interface is represented by

$$y = -\delta(x, t) \qquad [17]$$

where δ is a non-negative function. At any given time $t > 0$, this function will be different from zero in the region

$$x > -x_0(t) \qquad [18]$$

where $x = -x_0(t)$ is the position at which the interface meets the underside of the mask. Clearly, as etching proceeds, this point will move more and more to the left, *i.e.*, $x_0(t)$ is also a monotonically increasing function of the time. Next, we expect that, for any fixed value of x satisfying Eq. [18], the function δ will be monotonically increasing with time.

We shall consider here the simpler case of infinite reaction rate k_s, *i.e.*

$$c = 0 \quad \text{at} \quad y = -\delta(x, t) \qquad [19]$$

Clearly, the process is then diffusion controlled. The second condition corresponds to Eq. [8]. It describes the displacement of the boundary as a function of the concentration gradient. In more than one dimension, this condition is more complicated. The relevant analysis leading up to this condition is presented in the Appendix. Substituting $h = -\delta(x, t)$ in Eq. [A-5], we have

$$\frac{\partial \delta}{\partial t} = \sigma_e\left(\frac{\partial c}{\partial y} + \frac{\partial c}{\partial x}\frac{\partial \delta}{\partial x}\right) \quad \text{at } y = -\delta(x, t) \qquad [20]$$

The problem defined by Eq. [16], [19], and [20] and by the other relevant boundary conditions mentioned in the text was considered in (3), and an asymptotic solution valid for $\beta \gg 1$ was derived. However, the presentation of (3) emphasizes the applied mathematics aspects of the problem, so that the solution may not be directly accessible to the etching world. This is why we reconsider this problem here to emphasize the physical aspects of the analysis. Moreover, a knowledge of this solution is indispensable for a good understanding of the convective-diffusive case to be considered in the subsection that follows. Although it will be unavoidable to use some of the mathematics of (3), this will be kept to a minimum here.

The perturbation idea suggests that we might try to solve the present problem by first assuming δ to be zero for all t and $x > 0$. The next step is then to solve the resulting diffusion problem in the region with fixed boundaries ($y > 0$). Here, it is essential to realize that, during the first perturbation step, condition [19] is prescribed on $y = 0$ with $x > 0$.

This problem was solved in Ref. (3, 18). Because the interface is kept at its original position, the solution will be referred to as the reduced state. One of the more important results obtained in (3) is an expression for the normal concentration gradient at the interface, *i.e.*

$$\frac{\partial c}{\partial y} = \frac{c^b}{(Dt)^{1/2}} f\left(\frac{x^2}{8Dt}\right) \quad \text{at } y = 0 \quad (x > 0) \qquad [21]$$

where

$$f(z) = \frac{1}{\pi\sqrt{2\pi}} \left(e^{-z}K_{1/4}(z) + \int_0^z e^{-p}(K_{1/4}(p) + K_{3/4}(p))dp\right) \qquad [22]$$

The K-functions in Eq. [22] are modified Bessel functions (19).

A sketch of the function f is given in Fig. 7. From this figure, it is seen that f tends to a constant value when $z \gg 1$, *i.e.*, when x is much larger than the diffusion length $(Dt)^{1/2}$, which is far enough to the right of the mask edge. When the concentration gradient no longer depends upon x, the etching surface is expected to move downwards uniformly, *i.e.*, as a plane surface. Using the asymptotic form of f and substituting [21] in [20], we obtain, with $\partial\delta/\partial x = 0$

$$\frac{d\delta}{dt} = \frac{\sigma_e c^b}{(\pi Dt)^{1/2}} \qquad [23]$$

This may be integrated, subject to the initial conditions $\delta = 0$ at $t = 0$, to give

$$\delta = \frac{1}{\beta}\frac{2}{\pi^{1/2}}(Dt)^{1/2} \qquad [24]$$

which is the same as Eq. [14] for large values of β. This serves to show that etching is one-dimensional far enough from the mask edge, as expected.

When the argument of f is not particularly large, Fig. 7 shows that the normal gradient of c becomes larger, as we approach the mask edge. However, since we are considering small downward displacements, in full agreement with our perturbation assumptions, this will result in an etching profile that is only slightly curved. Therefore, $\partial\delta/\partial x \ll 1$ along most of the etching profile. As a result we may still approximate [20] by

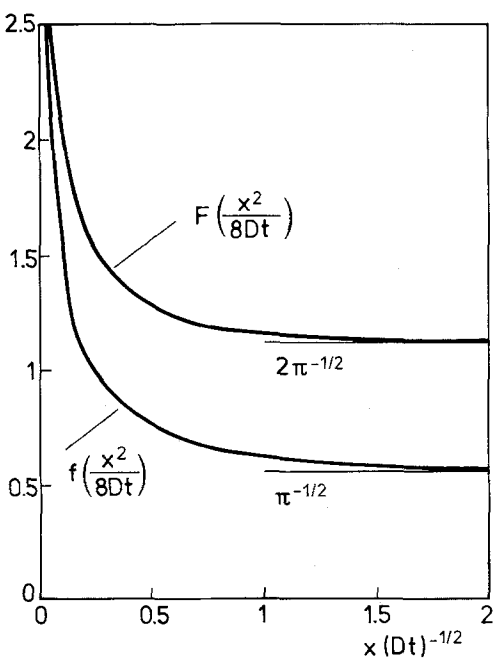

Fig. 7. Functions f (Eq. [22]) and F (Eq. [27]). These functions are proportional to surface mass transfer (f) and surface displacement (F) as predicted by the reduced state (see paragraph that includes Eq. [21]).

$$\frac{\partial\delta}{\partial t} \sim \sigma_e \frac{\partial c}{\partial y} \quad \text{at } y = 0 \qquad [25]$$

to obtain a first-order displacement of the etching surface. Integrating this equation, subject to $\delta = 0$ at $t = 0$, using Eq. [21], we obtain after some manipulation

$$\delta \sim \frac{(Dt)^{1/2}}{\beta} F\left(\frac{x^2}{8Dt}\right) \qquad [26]$$

where

$$F(z) = z^{1/2}\int_z^\infty \frac{f(q)}{q^{3/2}}\,dq \qquad [27]$$

This function is also presented in Fig. 7. Once again, this figure shows that the etching depth becomes uniform when $x \gg (Dt)^{1/2}$. When $x \sim (Dt)^{1/2}$, the argument is of order unity. Figure 7 and Eq. [26] show then that the etching depth is still of the order of the diffusion length divided by β, rendering a shallow etching profile. On the other hand, when the mask edge is approached so closely that $x \ll (Dt)^{1/2}$, the argument of F is almost zero. It can be shown that

$$F(z) \sim \frac{2^{3.4}}{3}\kappa z^{-1.4} + 1.047\, z^{1.4} + \ldots \qquad (0 < z \ll 1) \qquad [28]$$

where $\kappa = \Gamma(1/4)\pi^{-3/2} \sim 0.651$ is a constant that will appear more often in the present analysis (in Ref. (3) it is denoted by σ). This shows that, sufficiently close to the mask edge, the perturbation analysis, as we have applied it up to this point, breaks down. Clearly, one can no longer speak of small downward displacements of the etching surface when, at a given position x, the downward displacement δ is of the same order of magnitude as x itself. To see what values of x satisfy this condition, we substitute x for δ in Eq. [26]. Then, using Eq. [28] (leading term only), we find

$$\frac{x}{(Dt)^{1/2}} \text{ of the order of } \frac{1}{\beta}\left(\frac{x^2}{Dt}\right)^{-1.4} \qquad [29]$$

where some constants that are not essential in an order-of-magnitude analysis have been omitted. From [29], we conclude that the straightforward perturbation method breaks down when

$$x \text{ is of the order of } \beta^{-2.3}(Dt)^{1/2} \qquad [30]$$

Since the dimensionless parameter β is much larger than unity, the region defined by [30] is much smaller than the diffusion length.

To resolve this apparent difficulty, we must consider the full problem defined by Eq. [16], [19], and [20] and the other relevant boundary conditions in a relatively small region around the tip of the mask, the spatial extent of which is approximately that given by Eq. [30]. To that end, we introduce the scaled variables

$$X = \beta^{2.3}\frac{x}{(Dt)^{1/2}},\quad Y = \beta^{2.3}\frac{y}{(Dt)^{1/2}},$$

$$\Delta(X) = \beta^{2.3}\frac{\delta}{(Dt)^{1/2}} \qquad [31]$$

which blow up the aforementioned small region. The transformation of Eq. [31] could be considered as a mathematical magnifying glass. This way of looking at it is expressed pictorially in Fig. 8a and 8b. To be able to solve the field equations within the corner region around the tip of the mask (Fig. 8b), the original boundary condition at "infinity," which requires that $c \to c^b$, no longer applies. Referring to our earlier metaphor, we might say that the bulk of the etchant is far outside the range of the magnifying glass (Fig. 8a). Indeed, bulk conditions are reached at distances of at least a few diffusion lengths

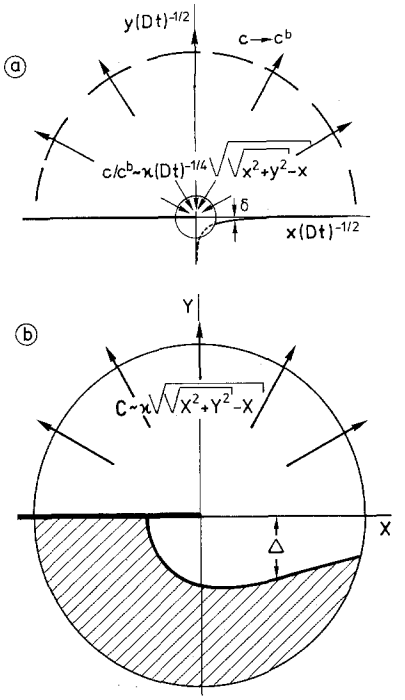

Fig. 8. The magnification of the corner region. This serves to show how the behavior of the reduced state close to the origin (a) determines the actual etching in the mask-edge region (b).

from the mask edge, whereas the size of the subregion is only of the order given by Eq. [30]. The conditions at the rim of the blown-up region are fully determined by the behavior of the reduced state (see text preceding Eq. [21]) close to the origin (Fig. 8a). This behavior may again be deduced from (3)

$$c \sim c^b \frac{\kappa}{(Dt)^{1/4}} \sqrt{(\sqrt{x^2 + y^2} - x)} \qquad [32]$$

It is interesting to note that [32] does indeed satisfy both the boundary condition on the mask and that on the stationary interface. Indeed, when $x > 0$, then c, as given by Eq. [32], is zero for $y = 0$, which is condition [19] for $\delta = 0$. Also, $\partial c/\partial y = 0$ holds when $x < 0$ and $y = 0$, which is the mask condition.

When the coordinate transformations of Eq. [31] are substituted in Eq. [32], it is easily seen that the field under the magnifying glass, the corner region of Ref. (3), is adequately described by the blown-up variable

$$C = \frac{c}{c^b} \beta^{1/3} \qquad [33]$$

The proper boundary conditions for C are then

$$\partial C/\partial Y = 0 \text{ (both sides of the mask)} \qquad [34]$$

$$C \to \kappa \sqrt{(\sqrt{X^2 + Y^2} - X)} \text{ when } X^2 + Y^2 \gg 1 \qquad [35]$$

and

$$C = 0 \text{ on } Y = -\Delta(X) \qquad [36]$$

Further, the displacement of the moving boundary, Δ, is now governed by the full Eq. [20]. This equation must be recast in terms of the scaled variables X, Y, C, and Δ using Eq. [31] and [33]

$$\Delta - X \frac{d\Delta}{dX} = 2 \left(\frac{\partial C}{\partial Y} + \frac{\partial C}{\partial X} \frac{d\Delta}{dX} \right) \text{ on } Y = -\Delta \qquad [37]$$

Although the boundary conditions are now far more complicated than those for the reduced problem, the governing differential equation is simpler than Eq. [16]. It is shown in (3) that the concentration field is quasi stationary in the corner region. It is governed by Laplace's equation

$$\frac{\partial^2 C}{\partial X^2} + \frac{\partial^2 C}{\partial Y^2} = 0 \qquad [38]$$

Consequently, the problem defined by Eq. [34]-[38] does not depend explicitly on time. Moreover, it does not contain any dimensionless physical parameters. The dependence upon β, in particular, has been scaled out. Therefore, the solution for the free boundary, $Y = -\Delta$, when found, applies to all relevant cases.

It is shown in (3) how a unique numerical solution for Δ may be obtained. The shape of the interface is given in Fig. 9. Furthermore, a pointwise representation is given in Table II. Of course, this solution for the interface applies in the magnified region. When the distance from the mask edge is no longer small in comparison with the diffusion length, Eq. [26] should be used. We refer to (3) for a method by which a smooth transfer from one solution to the other can be realized.

Some further important results are quoted here directly from (3). Denoting the lowest position of the etching profile by $(x, y) = (x_{bulge}, y_{bulge})$, we have

$$x_{bulge} \sim 0.370(Dt)^{1/2}\beta^{-1/3}; \; y_{bulge} \sim -0.720(Dt)^{1/2}\beta^{-2/3} \qquad [39]$$

Further, the underetching (see Fig. 6 and Eq. [18]) is given by

$$x_0 \sim 0.543(Dt)^{1/2}\beta^{-2/3} \qquad [40]$$

From Eq. [39] and [40], we obtain the important result

$$\text{etch factor} = \frac{|y_{bulge}|}{x_0} \sim 1.33 \qquad [41]$$

From the foregoing presentation it is clear that the shape of the etched profile remains unaltered during the entire etching process. However, as time proceeds, the profile in the corner region grows in proportion to the square root of the time, the magnification center being the tip of the mask.

The influence of convection.—We shall discuss the influence of convection in etching systems by studying a very simple model example. First, we shall assume that the velocity field in the liquid is given, *i.e.*, that it exists

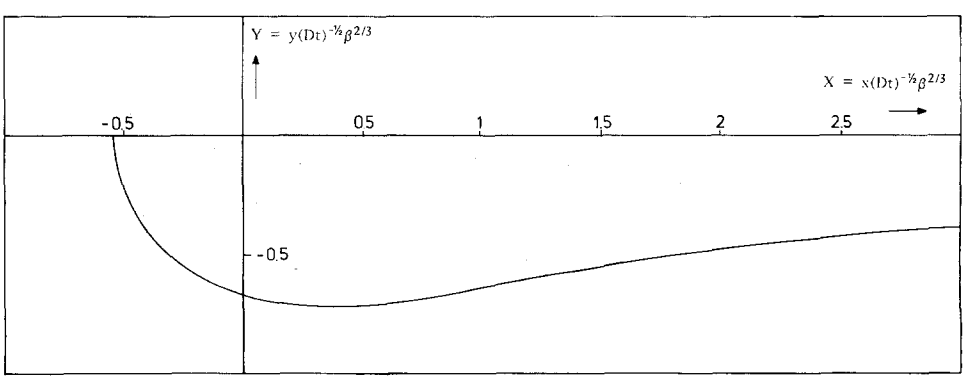

Fig. 9. The shape of the etching profile in the mask-edge region, as predicted by theory.

Table II. Position of the interface in purely time-dependent diffusion

$X = x(Dt)^{-1/2}\,\beta^{2/3}$	$Y = y(Dt)^{-1/2}\,\beta^{2/3}$
−0.543	0
−0.535	−0.104
−0.508	−0.206
−0.466	−0.303
−0.407	−0.395
−0.333	−0.479
−0.242	−0.551
−0.139	−0.613
−0.022	−0.662
0.106	−0.696
0.244	−0.715
0.391	−0.719
0.544	−0.712
0.703	−0.693
0.867	−0.665
1.036	−0.635
1.209	−0.602
1.389	−0.568
1.576	−0.536
1.769	−0.507
1.971	−0.480
2.40	−0.431
2.87	−0.391
3.37	−0.359
3.91	−0.330
4.50	−0.306
6.12	−0.259
8.00	−0.224
10.12	−0.198
12.50	−0.175
15.12	−0.160
18.0	−0.144
larger X	$-0.614\,X^{-1/2}$

independently of the etching process itself. This is a valid assumption when the etchant is stirred on purpose, as in jet or spray etching. On the other hand, even when very strict precautions are taken to ensure that the etchant remains stationary, etching itself induces stirring. Temperature or concentration differences caused by the etching process lead to density gradients, and these in turn give rise to the phenomenon of natural convection. Such flows have been studied in electrochemistry (20), crystal growth (21), and centrifugal etching (22). We shall not consider these more complicated situations here.

A further simplification is offered by the fact that the diffusive processes that tend to equalize existing velocity gradients are much stronger than those smoothing out concentration differences. As a result, concentration profiles are much sharper and more restricted in width than those of the velocity. To put it differently, if the full variation of the concentration from its bulk value at the etching surface (which is zero in this paper) occurs over a distance δ_c, the concentration boundary-layer thickness, then the velocity variations across this layer will only be minimal. For instance, at the solid wall (mask or interface), the velocity will have to be zero. Far enough from the wall, the velocity assumes a bulk value that is determined by the stirring conditions. However, at a distance δ_c from the wall, the velocity will have reached a level that is only a fraction of that of the bulk. As a result, a linearized velocity profile may be assumed to exist over the range δ_c from the wall into the etchant. This is the so-called Levêque approximation, which has been discussed extensively in the literature (23).

Simplifying our intended model still further, we shall assume that this linearized velocity profile is virtually independent of the coordinate that measures distance along the solid boundary. Referring to Fig. 6, this means a velocity field independent of the coordinate x. As long as the etching surface remains at its original position ($y = 0$), one can easily imagine such a velocity field to exist over some length, both toward the negative and the positive sides of the tip of the mask ($x = 0$, $y = 0$). However, when a profile has been etched, it is obvious that a complicated flow field will be set up in the underetched region (Fig. 10). It is our intention to show that, even in these circumstances, the linearized velocity model may sometimes be applied.

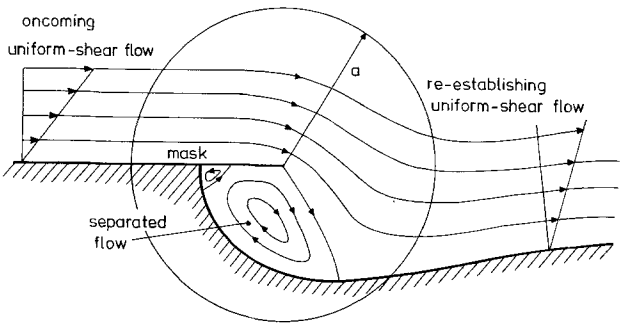

Fig. 10. A tentative view of the flow behavior of the etchant in the mask-edge region when a uniform shear flow is presented from the left. The radius a is defined by Eq. [56].

Under the simplified assumptions spelled out above, the transport of the active etching component is governed by

$$u\,\frac{\partial c}{\partial x} = D\left(\frac{\partial^2 c}{\partial x^2} + \frac{\partial^2 c}{\partial y^2}\right) \qquad [42]$$

where

$$u = u_0\,\frac{y}{\delta_u} \qquad [43]$$

is the linearized version of the velocity component in the x-direction. We use the geometry of Fig. 6. In Eq. [43], u_0 is the maximum velocity occurring in the system. Further δ_u is a measure of the thickness of the layer across which the velocity changes from zero to this maximum value (Fig. 11). Of course, Eq. [42] is used only when $y \lesssim \delta_c$, *i.e.*, within the concentration boundary layer. We have assumed that $\delta_c/\delta_u \ll 1$. In fact, it is shown in the literature (23, 24) that

$$\delta_c/\delta_u \sim \mathrm{Sc}^{-1/3} \qquad [44]$$

where the Schmidt number Sc is given by

$$\mathrm{Sc} = \nu/D \qquad [45]$$

Since the kinematic viscosity ν of a typical aqueous etchant is $\sim 10^{-6}$ m^2/s, we have Sc $\sim 10^3$, so that the ratio [44] is indeed small.

As explained in (23), Eq. [44] is, strictly speaking, valid only when the velocity field and the concentration field have developed over the same distance, *i.e.*, starting from the same point. In general, and certainly in the case we consider here, the velocity field is already fully developed in the region around the mask edge. If, as we shall assume, the direction of flow is from left to the right in Fig. 6, a fully developed velocity profile is presented at $x = 0$, whereas the concentration field only just begins

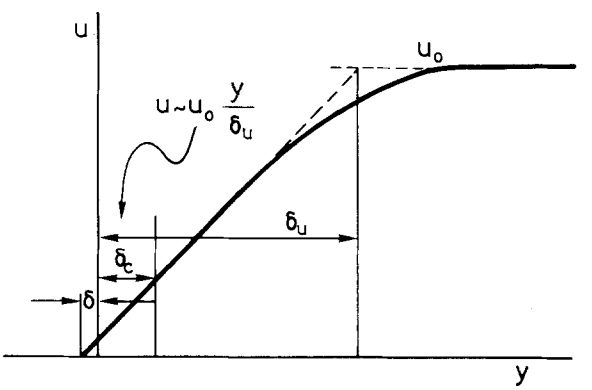

Fig. 11. Sketch showing the velocity profile along the etching surface (u) as a function of the normal coordinate (y). In the case depicted, the etching depth (δ) is much shallower than the thickness of the convection-diffusion layer (δ_c), which in its turn is always much thinner than the velocity layer (δ_u).

there. Under such conditions the ratio δ_c/δ_u may be much smaller than that given by Eq. [44].

The etching problem to be solved now is that governed by Eq. [42] and all the boundary conditions defined in the previous section. Of course, owing to the fact that the etching boundary moves, there is a time-dependent element in this problem that requires the addition of the term $\partial c/\partial t$ to the left side of [42]. However, since the motion of the boundary is very slow in comparison with the velocity of the etchant, this effect corresponds to a negligible quasi-stationary contribution. We shall again solve this problem with a perturbation technique, assuming that the concentration field may be calculated with the interface remaining at its original position in the plane $y = 0$ (Fig. 6). This is again referred to as the reduced state.

Introducing a characteristic length l based upon the physical parameters of Eq. [42]

$$l = \left(\frac{D\delta_u}{u_0}\right)^{1/2} \qquad [46]$$

we may define dimensionless variables as follows

$$\overline{X} = x/l, \overline{Y} = y/l, \overline{\Delta} = \delta/l, \overline{C} = c/c^b \qquad [47]$$

The reduced problem is now formulated by the equation

$$\overline{Y}\frac{\partial\overline{C}}{\partial\overline{X}} = \frac{\partial^2\overline{C}}{\partial\overline{X}^2} + \frac{\partial^2\overline{C}}{\partial\overline{Y}^2} \qquad [48]$$

with the boundary conditions

$$\text{at } \overline{Y} = 0 \begin{cases} \dfrac{\partial\overline{C}}{\partial\overline{Y}} = 0 \quad \text{if} \quad \overline{X} < 0 & [49] \\ \overline{C} = 0 \quad \text{if} \quad \overline{X} > 0 & [50] \end{cases}$$

and

$$\overline{C} \to 1 \quad \text{at} \quad \text{infinity} \qquad [51]$$

The solution to the problem defined by Eq. [48]-[51] can be found in (25). A particularly useful result that can be obtained from that reference is an expression for the concentration gradient at the boundary $Y = 0$ for $X > 0$. In that paper this gradient is denoted by the function $q(X)$. When we substitute this function in [20], remembering that for small displacements of the moving boundary, the term $\partial c/\partial y = c^b l^{-1}\,\partial\overline{C}/\partial\overline{X} = c^b l^{-1}\,q(\overline{X})$ dominates the right side, we may use Eq. [25] instead, and an expression for δ follows immediately

$$\delta = \frac{c^b\sigma_e}{l}\,q(\overline{X})t \qquad [52]$$

This shows that the etch rate is directly proportional to the time, as it should when fully developed conditions prevail.

It is also shown in (25) that $q(\overline{X})$ becomes unbounded when X tends to zero, *i.e.*, when the immediate neighborhood of the tip of the mask is approached. The behavior of $q(\overline{X})$ for small values of $\overline{X}$ reads

$$q(\overline{X}) \sim 0.44\,\overline{X}^{-1/2} \qquad [53]$$

As before, it will be reasonable to say that the straightforward perturbation procedure breaks down when δ becomes of the same order of magnitude as x, *i.e.*

$$\overline{X} \quad \text{of the order of} \quad \frac{1}{\beta}\frac{Dt}{l^2}\overline{X}^{-1/2} \qquad [54]$$

where we have used Eq. [13], [47], [52], and [53]. Consequently, the dimensions of the corner region are defined by

$$\overline{X} \quad \text{of the order of} \quad \beta^{-2/3}(Dt)^{2/3}l^{-4/3} \overset{\text{def}}{=} A \qquad [55]$$

In the dimensional plane, this defines a region with a radius of the order of (see Fig. 10)

$$(x^2 + y^2)^{1/2} \sim lA \overset{\text{def}}{=} a \qquad [56]$$

Although Eq. [55] is quite similar to Eq. [30], there is an important difference between the analysis of this section and that of the previous one. In the foregoing section, the concentration field was diffusive; its spatial extent was determined by the diffusion length everywhere and at all times. Therefore, and since $\beta \gg 1$, the region defined by [30], as expressed by the transformation of Eq. [31], is always a small subregion within the whole field (Fig. 8). The problem defined by Eq. [48]-[51], on the other hand, refers to a spatial domain that does not grow in time, since steady-state conditions have been assumed from the outset. Within such a stationary field, the subregion suggested by [55] or [56] may indeed be small at first. However, as soon as $A \approx 1$, *i.e.*, when Dt is of the order of βl^2, one may no longer speak of a subregion. Once again referring to our earlier metaphor: the magnifying glass loses its power after some time.

Assuming that the etching time is still small enough for Eq. [55] to define a proper subregion, we proceed by introducing the transformation

$$(\tilde{X}, \tilde{Y}, \tilde{\Delta}(\tilde{X})) = \epsilon A^{-1}(\overline{X}, \overline{Y}, \overline{\Delta}(\overline{X})) \qquad [57]$$

which blows up the $(\overline{X}, \overline{Y})$ domain along the same lines as shown in Fig. 8. The dimensionless numerical constant ϵ will be determined in the course of the analysis. Next, it can be shown from the analysis of (25) that

$$\overline{C} \sim 0.62\sqrt{(\sqrt{\overline{X}^2 + \overline{Y}^2} - \overline{X})} \qquad [58]$$

when $\overline{X}_2 + (Y_2 \ll 1$ (the constant $0.62 \sim 0.44\sqrt{2}$). Equations [35], [57], and [58] suggest that we introduce

$$\tilde{C}(\tilde{X}, \tilde{Y}) = \frac{\kappa}{0.62}\epsilon^{1/2}A^{-1/2}\overline{C}(\overline{X}, \overline{Y}) \qquad [59]$$

in addition to [57]. Substituting Eq. [57] and [59] in Eq. [48]-[50] and [58], we obtain the following set of equations and boundary conditions

$$\frac{\partial^2\tilde{C}}{\partial\tilde{X}^2} + \frac{\partial^2\tilde{C}}{\partial\tilde{Y}^2} = \epsilon^{-2}A_2\tilde{Y}\frac{\partial\tilde{C}}{\partial\tilde{X}} \qquad [60]$$

$$\frac{\partial\tilde{C}}{\partial\tilde{Y}} = 0 \quad \text{on the mask (both sides)} \qquad [61]$$

$$\tilde{C} = 0 \quad \text{on} \quad \tilde{Y} = -\tilde{\Delta} \qquad [62]$$

and

$$\tilde{C} \to \kappa\sqrt{(\sqrt{\tilde{X}^2 + \tilde{Y}^2} - \tilde{X})} \quad \text{when} \quad \tilde{X}^2 + \tilde{Y}^2 \gg 1 \qquad [63]$$

Moreover, transforming Eq. [20] with the aid of Eq. [47] and [57], we may derive

$$\tilde{\Delta} - \tilde{X}\frac{d\tilde{\Delta}}{d\tilde{X}} = \frac{3(0.62)}{2\kappa}\epsilon^{3/2}\left(\frac{\partial\tilde{C}}{\partial\tilde{Y}} + \frac{\partial\tilde{C}}{\partial\tilde{X}}\frac{d\tilde{\Delta}}{d\tilde{X}}\right) \qquad [64]$$

The availability of the free constant ϵ in Eq. [64] enables us to render the coefficient of the right side of [64] equal to 2, as in Eq. [37]

$$\epsilon = \left(\frac{4\kappa}{3(0.62)}\right)^{2/3} = 1.25 \qquad [65]$$

The system of equations and boundary conditions [60]-[64] is almost the same as that of Eq. [34]-[38]. The only difference still remaining is that between Eq. [38] and [60]. However, as long as $A \ll 1$, *i.e.*, when

$$Dt \ll \beta l^2 \qquad [66]$$

the right side of [60] may be disregarded, and a complete analogy between the analysis of the present and the previous sections follows with regard to the behavior near the mask edge.

The results of the present analysis may now be summarized. As long as [66] is valid, the etching profile in the corner region around the mask edge will be approximately that given by Fig. 9 and Table II, where the wriggled variables of this section may be identified with the variables denoted by capitals in the previous section. The etch factor will be 1.33, as before. Furthermore, the position of the bulge will be at

$$x_{\text{bulge}} = 0.296(Dt)^{2/3}l^{-1/3}\beta^{-2/3};$$

$$y_{\text{bulge}} = -0.576(Dt)^{2/3}l^{-1/3}\beta^{-2/3} \quad [67]$$

Of course, outside the mask-edge region, the etching depth determined in the present section [52] is totally different from that given by [26] for a purely diffusive field. Whereas, in purely diffusive transport, the bulge near the tip of the mask will never disappear, since the ratio of etching depths near the mask and far away from it is always of the order of $\beta^{1/3}$, this special behavior of the etching profile will become less and less marked as time proceeds in the case of convective-diffusive transport. Indeed, taking the ratio of y_{bulge} (Eq. [67]) and δ (Eq. [52]), we obtain the following order-of-magnitude expression

$$\frac{|y_{\text{bulge}}|}{\delta(\overline{X} \text{ order unity})} \sim l^{2/3}\beta^{1/3}(Dt)^{-1/3} \quad [68]$$

As long as Eq. [66] is valid, this ratio is large, which shows that a bulge will be seen near the mask edge. At longer times, the mask-edge region merges more and more with the field elsewhere, and the complete problem has to be solved. This means that the convection term can then no longer be disregarded in the mask region. The complete Navier-Stokes system must then be tackled to calculate the influence of convection.

Conclusions

In this paper, we have shown that it is possible to devise simple mathematical models which predict certain etching results that have been observed in practice. On the basis of a straightforward one-dimensional model, we have demonstrated that a dimensionless parameter β (Eq. [13] and [15]) determines particular etching processes to a large extent. We estimated the value of β for a number of example systems and found this parameter to be always much larger than unity. From this, we deduced that the displacement of the etching boundary is relatively slow. This fact suggested that etching models can be solved by so-called perturbation techniques, by which one may calculate the concentration field assuming the interface to remain fixed at its original position. From this, we were able to obtain a first-order displacement of the interface.

The perturbation technique was then applied to a mathematical model that we devised for the etching of a semi-infinite solid that was partly covered with a mask. Several observations reported in the literature (6, 7, 8) show that etch rates may be much higher near the resist edge than further away from this edge. In all cases, these processes were diffusion-controlled. Although it was suggested at first that surface diffusion of adsorbed ions along the mask might be responsible, a rough model (7) showed that enhanced bulk diffusion near the edge must be the true cause. This observation is now confirmed by our more sophisticated time-dependent model, which actually leads to a description of the resulting curved interface. This calculated interface (Fig. 9 and Table II) reveals a relatively deep trough in the immediate vicinity of the resist edge.

When convection is totally absent, the etch rate near the mask edge is larger than that far away from the edge by a factor that is of the order of $\beta^{1/3}$. Therefore, although the etch rate decreases as β increases, the ratio of etch rates increases with β. Therefore, if one wishes to etch out a circular area from a thin substrate, one might save active etching component by increasing the value of β. This could be achieved by lowering the concentration c^b. Of course, one will have to pay for this by having to wait longer for the final result. It should be realized that this observation is valid only as long as the diffusion length is small in comparison with the diameter of the region to be etched out.

Since convection can hardly ever be suppressed in practice — on the contrary, it is almost invariably a dominant factor — we investigated its influence on etching near the mask edge. Again, we found a bulging shape of the interface near the mask edge. Moreover, for sufficiently shallow etching results, the shape was shown to be exactly the same as that derived for the case of a quiescent etchant. This is of importance experimentally. It shows that slight convection levels can be allowed that all lead to a single definite result, viz., that observed in a stationary etchant.

Although a qualitative agreement has now been shown to exist between actual experimental observations and our mathematical model, it still remains to be seen whether the predicted shape (Fig. 9) can be confirmed experimentally. This will be the subject of our next paper (9).

Manuscript received April 22, 1985.

Philips Research Laboratories assisted in meeting the publication costs of this article.

APPENDIX

The Moving Boundary Condition in More Than One Dimension

Let us consider Fig. A-1, which shows two corresponding contiguous parts of the moving boundary at the times t and $t + \Delta t$, respectively, where Δt is assumed to be a small time increment. The moving boundary is denoted by $y = h(x, t)$. According to the sketch as given in the figure, the etchant is to be found above the moving boundary, and the solid below it. If the velocity of the moving boundary in the direction of the inward normal n is denoted by v_n, the moving boundary condition in its simplest form relates this velocity to the normal gradient of c as follows

$$v_n = -\sigma_e \frac{\partial c}{\partial n} \quad [A\text{-}1]$$

The minus sign must be chosen, since we have assumed that c is the concentration of the active etching component. Indeed, the moving boundary being a sink with respect to the active component, the concentration will be lowest there. As a result, the gradient will be positive in the direction of negative n.

By considering the tangent of the moving boundary at A (see Fig. A-1), we may express the normal gradient in terms of the derivative with respect to x and y as follows

$$\frac{\partial c}{\partial n} = \frac{\partial c}{\partial x}\frac{\partial x}{\partial n} + \frac{\partial c}{\partial y}\frac{\partial y}{\partial n} = \frac{\partial c}{\partial x}\sin\phi - \frac{\partial c}{\partial y}\cos\phi \quad [A\text{-}2]$$

with

$$\tan\phi = \frac{\partial h}{\partial x} \quad [A\text{-}3]$$

The length of section AB is approximately equal to $-(\partial h/\partial t)\Delta t$. Hence, the normal velocity of the moving boundary is given by

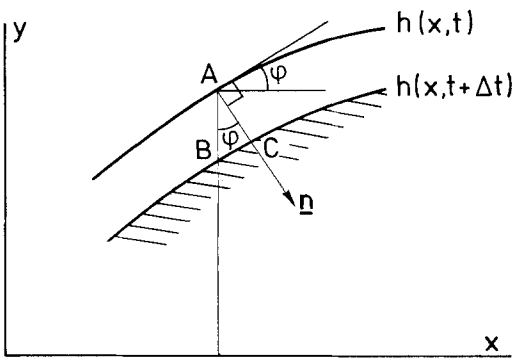

Fig. A-1. Sketch to be used in the derivation of the etching boundary condition of Eq. [A-10].

$$v_n \sim \frac{AC}{\Delta t} = \frac{AB \cos \phi}{\Delta t} = -\frac{\partial h}{\partial t} \cos \phi \qquad [A\text{-}4]$$

From Eq. [A-1]-[A-4], we may finally deduce

$$\frac{\partial h}{\partial t} = -\sigma_e \left(\frac{\partial c}{\partial y} - \frac{\partial c}{\partial x} \frac{\partial h}{\partial x} \right) \quad \text{at} \quad y = h(x, t) \qquad [A\text{-}5]$$

as the moving boundary condition in two dimensions.

Considering the problem in three dimensions, *i.e.*, assuming $y = h(x, z, t)$, where z is the coordinate normal to both x and y, we may derive similarly

$$\frac{\partial h}{\partial t} = -\sigma_e \left(\frac{\partial c}{\partial y} - \frac{\partial c}{\partial x} \frac{\partial h}{\partial x} - \frac{\partial c}{\partial z} \frac{\partial h}{\partial z} \right) \quad \text{at} \quad y = h(x, z, t) \qquad [A\text{-}6]$$

REFERENCES

1. D. W. Shaw, *J. Cryst. Growth*, **47,** 509 (1979).
2. D. W. Shaw, *This Journal*, **128,** 874 (1981).
3. H. K. Kuiken, *Proc. R. Soc., London, Ser. A.*, **392,** 199 (1984).
4. H. K. Kuiken, *ibid.*, **396,** 95 (1984).
5. C. Vuik and C. Cuvelier, *J. Comp. Phys.* (1985).
6. D. W. Shaw, *This Journal*, **113,** 958 (1966).
7. W. G. Oldham and R. Holmstein, *ibid.*, **114,** 381 (1967).
8. E. Kohn, *ibid.*, **127,** 505 (1980).
9. P. H. L. Notten, J. J. Kelly, and H. K. Kuiken, *ibid.*, **133,** 1226 (1986).
10. H. Gerischer and W. Mindt, *Electrochim. Acta*, **13,** 1329 (1968).
11. H. Gerischer and I. Wallem-Mattes, *Z. Phys. Chem., N.F.*, **64,** 187 (1969).
12. P. H. L. Notten, *This Journal*, **131,** 2641 (1984).
13. E. Haroutounian, J.-P. Sandino, P. Cléchet, D. Lamouche, and J.-R. Martin, *ibid.*, **131,** 27 (1984).
14. J. O'M. Bockris and D. M. Drazic, "Electro-Chemical Science," Chap. 4, Taylor & Francis, London (1972).
15. J. R. Ockendon and W. R. Hodgkins, "Moving Boundary Problems in Heat Flow and Diffusion," p. 120, Clarendon, Oxford (1975).
16. J. Crank, "Free and Moving Boundary Problems," p. 1, Clarendon, Oxford (1984).
17. D. D. MacDonald, "Transient Techniques in Electrochemistry," Chap. 4.3, Plenum Press, New York (1977).
18. K. B. Oldham, *J. Electroanal. Chem.*, **122,** 1 (1981).
19. M. Abramowitz and I. A. Stegun, "Handbook of Mathematical Functions," p. 374, Dover, New York (1965).
20. J. R. Selman and J. Newman, *This Journal*, **118,** 1070 (1971).
21. W. van Erk and H. K. Kuiken, *J. Cryst. Growth*, **51,** 397 (1981).
22. H. K. Kuiken and R. P. Tijburg, *This Journal*, **130,** 1722 (1983).
23. V. G. Levich, "Physicochemical Hydrodynamics," Chap. 2, Prentice Hall, Englewood Cliffs, NJ (1962).
24. R. B. Bird, W. E. Stewart, and E. N. Lightfoot, "Transport Phenomena," John Wiley and Sons, New York (1960).
25. S. G. Springer and T. J. Pedley, *Proc. R. Soc., London, Ser. A*, **333,** 347 (1973).
26. H. Gerischer, *Ber. Bunsenges. Phys. Chem.*, **69,** 578 (1965).
27. W. Kern, *R.C.A. Rev.*, **39,** 278 (1978).
28. G. Gerlagh and P. Baeyens, *Trans. Inst. Met. Finishing*, **53,** 133 (1975).
29. W. Kern, in "Etching for Pattern Definition," H. G. Hughes and M. J. Rand, Editors, p. 1, The Electrochemical Society Softbound Proceedings Series, Princeton, NJ (1976).

Etching Profiles at Resist Edges

II. Experimental Confirmation of Models Using GaAs

P. H. L. Notten, J. J. Kelly, and H. K. Kuiken

Philips Research Laboratories, 5600 JA Eindhoven, The Netherlands

ABSTRACT

Etching experiments have been carried out with GaAs in order to check mathematical models developed for diffusion-controlled dissolution at resist edges. Both electroless and chemical etchants were used, and their chemistry is briefly considered. An interesting method of controlling the electroless dissolution rate of GaAs by means of a diffusion-controlled oxidation reaction is reported. The excellent agreement between calculated and measured etched profiles demonstrates the validity of the mathematical model. The influence of natural convection and of convection induced by gas evolution is reported, and the results are compared with theory.

In Part I (1) a mathematical model was presented to describe diffusion-controlled etching at resist edges. Both the form of the etched profiles and the characteristics of the etching kinetics at the edges are predicted by the model.

In the present paper we attempt to verify the model experimentally. In order to do this, we need etching systems that meet two main requirements (1). (*i*) The etch rate on all crystal planes of the solid must be determined by mass-transport in the solution, *i.e.*, the rate constant for the rate-determining step of the dissolution process must be sufficiently large to ensure a very low surface concentration of the rate-determining species, even at the slowest etching plane. (*ii*) The dimensionless etching parameter β, introduced in Part I to describe the dissolution process, must be large (≥ 100).

Etching methods not involving an external current or voltage source can be divided into two classes: electroless and chemical (2). Electroless etching occurs at a well-defined mixed potential that is determined by two potential-dependent electrochemical reactions; at this potential, the rates of dissolution of the solid and reduction of the oxidizing agent in the solution are equal. Chemical dissolution is observed with bifunctional molecules that are capable of forming new bonds with two neighboring surface atoms simultaneously. The etch rate, in this case, does not depend on the surface concentration of charge carriers in the solid and is not influenced by an externally applied potential (3).

As a model system in the present work, the etching of GaAs, which is very important for device applications, was considered. This material can be dissolved with both electroless and chemical etchants. In order to decide on how to comply with the requirements of the mathematical model, we examined the chemistry of possible etching systems. Apart from the two requirements described above, the precise etching mechanism is important in determining the etched profiles. For this reason, we first consider briefly the mechanism of electroless and chemical dissolution of GaAs. Results obtained experimentally with suitable etchants are then described and compared with those predicted by theory.